



Pergamon

Tetrahedron 55 (1999) 14961–14974

TETRAHEDRON

**Acyclic Phenylalkanedioles as Substrates for the Study of Enzyme Recognition.  
Regioselective Acylation by Porcine Pancreatic Lipase: A Structural Hypothesis for the  
Enzymatic Selectivity**

Isabel Borreguero<sup>a</sup>, José V. Sinisterra<sup>a</sup>, Angel Rumbero<sup>b</sup>, Juan A. Hermoso<sup>c</sup>, Martín Martínez-Ripoll<sup>f</sup> and Andrés R. Alcántara<sup>\*\*</sup>

<sup>a</sup> Departamento de Química Orgánica y Farmacéutica. Facultad de Farmacia. Universidad Complutense, 28040 Madrid (Spain).  
Phone no. +34-913941820. Fax no. +34-913941822.

<sup>b</sup> Departamento de Química Orgánica. Facultad de Ciencias. Universidad Autónoma, Cantoblanco. 28049-Madrid (Spain).

<sup>c</sup> Grupo de Cristalografía Macromolecular y Biología Estructural. Instituto de Química Física "Rocasolano". Serrano 119. 28008 Madrid (Spain)

Received 26 July 1999; revised 29 September 1999; accepted 14 October 1999

**Abstract**

The regioselective acylation of phenylalkanedioles catalysed by porcine pancreatic lipase (PPL) was the reaction used for modelling different areas in the active site of the enzyme. With this aim, different racemic or prochiral (*1,n*)-diols, with *n* ranging from 2 to 6 were resolved *via* transesterification with vinyl acetate, and the results were explained according to microcrystalline enzyme structure. Thus, we describe a logical model for explaining the enzyme regio and stereoselectivity, based on three residues of the active site (Ser153, Phe216 and His264) which turned out to be crucial for the substrate binding and transformation. © 1999 Elsevier Science Ltd. All rights reserved.

**Keywords:** Phenylalkanedioles; Porcine Pancreatic Lipase; Transesterification; Active site model; Substrate binding.

**Introduction**

Lipase-mediated resolution of chiral alcohols, either by acyl transfer methods or by hydrolysis of their corresponding esters, is probably the biotransformation most commonly described in modern literature.<sup>1-3</sup> When the substrate presents two reactive centres for the lipase action (diols), the possibility of exploiting both the regio and the enantioselectivity of the biocatalyst makes the process even more attractive. When using diols containing a primary and a secondary alcohol, the primary hydroxyl group is resolved much faster than the secondary, which generally remains unaltered.<sup>4-6</sup> On the other hand, if the lipase has to distinguish between two primary hydroxyl groups, the observed enantiomeric excess normally is high for prochiral diols,<sup>7</sup> although only moderate for racemic mixtures.<sup>8</sup> In the discrimination between two secondary hydroxyl functions placed in the same molecule, once again the reported stereobias generally is acceptable for meso,<sup>9,10</sup> or prochiral diols,<sup>7,11,12</sup> although some *meso* diols are described as very poor substrates for enzyme-catalysed transesterification with vinyl acetate.<sup>13</sup>

There are several references in the lipase literature that propose some empirical rules for the prediction of the enantiopreference of different lipases on chiral alcohols, based either on the relative site of the substituents around the substrate stereocentre or by simply defining a "box" for the enzyme binding site and fitting inside the respective substrates, secondary<sup>14,16</sup> or primary alcohols.<sup>17-19</sup> More recently, some structural basis for explaining these

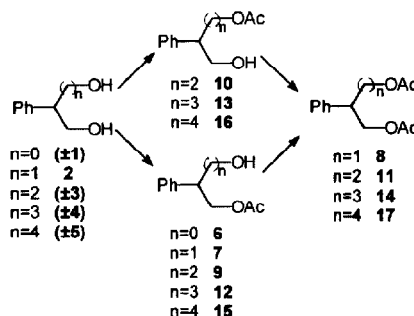
\*Corresponding author: andresr@eucmax.sim.ucm.

empirical rules have been published: thus, by studying the 3D structure of *Candida rugosa* lipase (CRL) complexed with transition-state mimicking inhibitors (determined by X-ray diffraction), Cygler *et al.*<sup>20</sup> found that the alcohol binding site of CRL resembled the rule predicted for secondary alcohols, and Uppenberg *et al.*<sup>21</sup> showed the stereospecific pocket for the recognition of secondary alcohols in the structure of *Candida antarctica* lipase B. Other suggestions for understanding lipase enantioselectivity come from the field of molecular modelling: thus, Hult and coworkers<sup>22–24</sup> explained the basis for the enantioselective recognition of substrates of CRL<sup>22,23</sup> and lipase B from *Candida antarctica*,<sup>24</sup> and also molecular modelling was used by Zuegg *et al.*<sup>25</sup> in the study of the selectivity of lipases from *Candida rugosa* and *Pseudomonas cepacia* on secondary and primary alcohols, while Grabuleda *et al.*<sup>16</sup> recently developed a three-pocket model for explaining the enantioselectivity pattern of secondary alcohols inside the active site of *Pseudomonas cepacia* lipase.

Nevertheless, the rules proposed for explaining the stereobias of PPL on primary alcohols are not very convincing, even considering the relative hydrophobicity or polarity of substrate moieties, and the controversy exists because enantiomeric models are proposed.<sup>26–28</sup> Recently, the crystal structure of the ternary complex porcine lipase-colipase-tetraethylene glycol monoethyl ether (TGME) has been determined by X-ray diffraction at 2.8 Å resolution.<sup>29,30</sup> In this paper we present the results obtained in the resolution of 1,*n*-diols (*n*=2,3,4,5,6) by means of PPL-catalysed transesterification with vinyl acetate. The regio and enantioselectivity is discussed with reference to the active site model based on the crystalline enzyme structure. This qualitative model enables a rational explanation of the enzymatic stereocontrol at a higher level than other previously proposed models.<sup>17,26–28</sup>

## Results and Discussion

In this paper we describe the transesterification of several (1, *n*)-diols, as shown in Scheme 1: racemic phenyl-1,2-ethanediol ((±)-1, commercially available substrate, *n*=2); 2-phenyl-1,3-propanediol (2, prochiral compound, *n*=3) and racemic 2-phenyl-1,4-butanediol ((±)-3, *n*=4), which were prepared from diethyl phenylmalonate and diethyl 2-phenylsuccinate respectively, as described elsewhere<sup>31</sup>; and finally, two racemic acyclic diols, 2-phenyl-1,5-pentanediol, (±)-4 (*n*=5) and 2-phenyl-1,6-hexanediol (±)-5 (*n*=6), whose synthesis has been previously described.<sup>31</sup> The determination of the enantiomeric purity of reaction products (monoacetates and diacetates) and remaining diols, the sign of the optical rotation of the enantiomers, as well as the absolute configuration of the compounds were established by different methods as described elsewhere.<sup>31</sup>



Scheme 1. Overall reaction scheme.

### Resolution of racemic phenylethan-1,2-diol (±1)

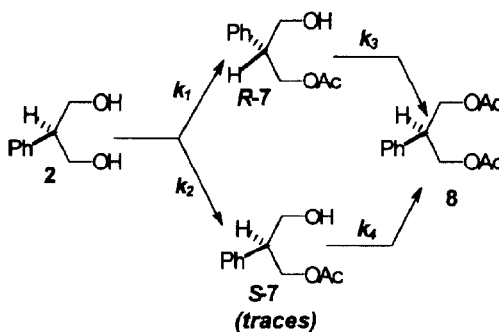
Different compounds possessing the 1, 2-diol functionality are useful as synthetic intermediates,<sup>8</sup> drugs and pharmaceutical intermediates.<sup>32,33</sup> Therefore, some enantioselective chemical methods for the preparation of these

compounds have been described in the literature.<sup>34–36</sup> The enzymatic preparation of homochiral 1, 2-diols have also been reported, following different strategies: lipase-catalysed kinetic resolution of racemic 2-hydroxy carboxylic esters followed by a reduction step,<sup>37</sup> lipase-catalysed transesterification (or hydrolysis) of monoprotected diols (or their corresponding acylated compounds),<sup>4, 38, 39</sup> by means of a lipase-catalysed alcoholysis of the diacylated diols,<sup>40</sup> or more recently by enantioselective epoxide-hydrolases.<sup>41, 42</sup> When using an enzyme for the enantioselective acylation of racemic diols, Theil<sup>43</sup> considered two main cases, which can be treated as reactions of monohydroxy compounds: the first case involves reaction termination after the first acylation step,<sup>44, 45</sup> while, in the second case, this first acylation step quickly leads (with low enantioselectivity) to the corresponding racemic monoacetate, which is a better substrate for the enzymatic catalysis, therefore obtaining (with better enantioselectivity) a monoacylated derivative and the corresponding diacylated compound.<sup>46, 47</sup>

In the enzymatic resolution of ( $\pm$ )-**1** only the monoacetate **6** (with low optical purity, ee around 20%) was detected, with no traces of any other monoacetate (acylation on the secondary OH) or diacetate. Therefore, this absolutely regioselective process should be considered as belonging to the above-mentioned Theil's first case reactions.

### Desymmetrisation of 2-phenyl-1,3-propanediol (**2**)

Prochiral diols (*meso*-compounds or molecules possessing pseudo-asymmetric centres) are very useful synthetic intermediates because the maximum feasible yield upon its enzymatic transformation is not limited to 50%, as happens when resolving racemic mixtures. 2-substituted 1,3-propanediols have been extensively used in lipase-



Scheme 2. Kinetic resolution of **2**

catalysed acylation, due to their synthetic flexibility.<sup>36</sup> Thus, many references can be found in literature covering the PPL-catalysed desymmetrisation of these compounds.<sup>7, 12, 48–50</sup>

In Figure 1 we present the progress curve obtained in the acylation of 2-phenyl-1, 3-propanediol (**2**) with vinyl acetate, and the results are summarized in Scheme 2. This acylation showed a

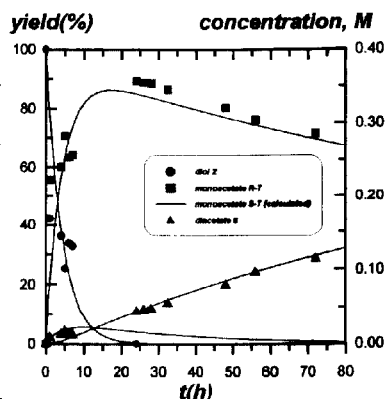


Figure 1. Progress curve of the PPL-catalysed transesterification of **2** with vinyl acetate. Consumption of **2** and formation of *R*-**7**, *S*-**7** (calculated according to Eq. 3) and **8**. Conditions as described in Experimental Section.

high *R*-stereopreference in the monoacylation (*ee* >95% *R*-monoacetate *R*-7), detecting only traces (<5% of *S*-monoacetate *S*-7), in agreement with the data reported in the literature.<sup>43</sup> Compound 2 is more reactive than the racemic diol ( $\pm$ )-1, because the prochiral compound is completely consumed after 24 hours, while 40% of ( $\pm$ )-1 remains unaltered after 80 hours, and also the enantiopurity obtained is higher. On the other hand, *R*-7 could be considered as an unstable primary compound, following the classical nomenclature of Campbell and Wojciechowski,<sup>51</sup> because it is produced from the earlier reaction steps and consumed as the reaction progresses, as deduced from the slow decrease of its concentration at  $t > 20$  h; the diacetate 8, using the same above-mentioned nomenclature, is a stable primary compound because it is produced from the very beginning of the reaction, and its yield increases with the reaction time. Therefore we must conclude that *R*-7 and 8 are consecutively produced, but the first acylation is faster than the production of 8.

#### Acylation of 2-Phenyl-1, 4-butanediol ( $\pm$ )-3, 2-phenyl-1, 5-pentanediol ( $\pm$ )-4 and 2-phenyl-1, 6-hexanediol ( $\pm$ )-5.

The resolution of racemic acyclic ( $1, n$ )-diols, with  $n > 3$ , is not very well documented. So, despite the many references found in the literature dealing with the asymmetrisation of:

- i) cyclic primary *meso*-diols,<sup>52–54</sup>
- ii) cyclic (generally six and seven-membered cycles) secondary *meso*-diols,<sup>55–57</sup> or even
- iii) acyclic *meso*-diols<sup>58–60</sup> in which

both hydroxy groups are separated by more than two carbon atoms, the resolution of these “long-distance” racemic diols has only been studied in depth for cyclic compounds.<sup>61,62</sup> Very little is described about the resolution of such racemic acyclic diols;<sup>63,64</sup> the resolution of 2-phenyl-1, 4-butanediol ( $\pm$ )-3, 2-phenyl-1, 5-pentanediol ( $\pm$ )-4 and 2-phenyl-1, 6-hexanediol ( $\pm$ )-5 constitutes a good approximation to this subject.

First, these diols were synthesized as described in a previous paper,<sup>31</sup> and subsequently used as substrates for the PPL-catalysed acylation with vinyl acetate. The reaction progress was

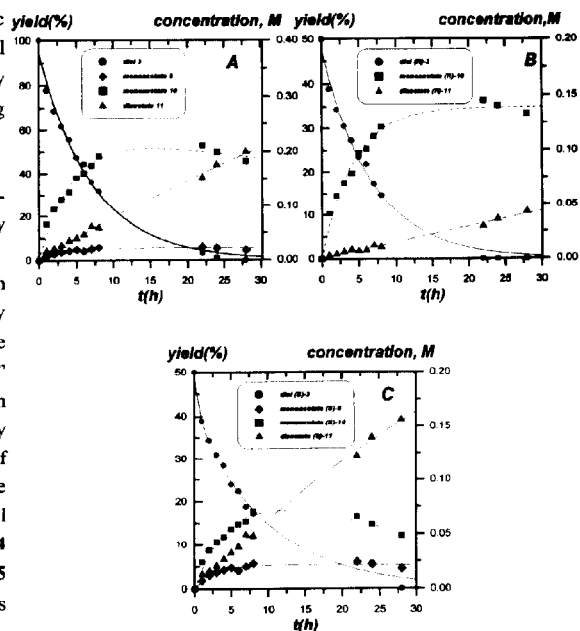
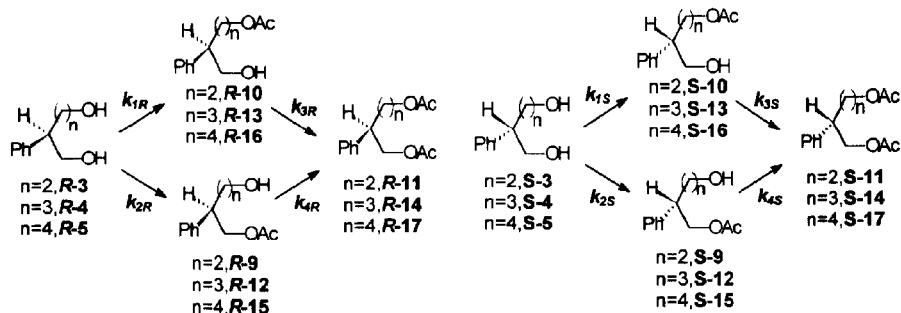


**Figure 2.** Progress curves of the PPL-catalysed transesterification of ( $\pm$ )-3 with vinyl acetate. (A) Consumption of ( $\pm$ )-3 and formation of 9, 10 and 11. (B) Consumption of *R*-3 and formation of *S*-9 and *R*-11. (C) Consumption of *S*-3 and formation of *S*-9, *S*-10 and *S*-11. Conditions as described in Experimental Section.

followed by chiral HPLC (See Experimental Section). Figure 2 shows the results obtained for the acylation of ( $\pm$ )-3 (for ( $\pm$ )-4 and ( $\pm$ )-5 similar curves were obtained (not shown)). For simplifying the understanding of the PPL enantioselection over the starting racemic materials, the consumption of the corresponding *R*-diol and the formation of the *R*-products is presented in Figure 2B, while in Figure 2C similar curves are displayed for the *S*-counterparts. In all cases, the regioselective acylation in the primary hydroxy group which is further from the stereocentre is the main process, yielding the monoacetates (major products) 10, 13, and 16 (see Scheme 1), which are primary compounds, with slight *R*-stereopreference, although this decreases as going from the 1,4 to the 1,6-diol.

On the other hand, the acylation of the primary hydroxy group that is closer to the stereogenic centre renders the “minor” monoacetates 9, 12 and 15, in lower yields compared to the major compounds, although with higher optical purity (*S*-stereopreference, with no traces of the *R*-compounds except for 15). These primary compounds (major and minor monoacetates) undergo a second acylation in their free -OH groups, leading to the *S*-enriched diacetates 11, 14 and 17. Only in the acylation of ( $\pm$ )-3, the concentration of the major monoacetate ( $\pm$ )-10 slightly decreases with the reaction time (Fig.2A), which is mainly due to the *S*-10 transformation into *S*-11 (Fig. 2C), because *R*-10 remains unaltered at high reaction time (Fig. 2B) In the other diols ( $\pm$ )-4 and ( $\pm$ )-5, both major monoacetates achieve a stable yield (~ 55-60%). Thus, comparing the global reactivity of ( $\pm$ )-3, ( $\pm$ )-4 and ( $\pm$ )-5 with ( $\pm$ )-1 and 2, we deduced this relative activity: 2 > ( $\pm$ )-3, ( $\pm$ )-4, ( $\pm$ )-5 >> ( $\pm$ )-1. From all these curves, we can postulate the reaction scheme depicted in Scheme 3, where two similar pathways are defined for the *R* and the *S* enantiomers. In all cases, the *R*-isomer undergoes the first acylation faster than the *S*-antipode, leading to greater yields of *R*- monoacetate than of *S*-monoacetate; on the other hand, the *R*-diol is not acylated in the short chain, except for the 1,6-diol. This finding indicates that some steric restrictions may exist around this hydroxyl group when the substrates are approaching the active site. In the second reaction step, the monoacetates 10, 13 and 16 are acylated again, with the *S*-monoacetate transformed faster than its *R*-counterpart for all cases. Finally, the minor monoacetates, 9, 12 and 15, produced by acylation in the short chain, seem to be resistant to the second acylation.



Scheme 3. Kinetic resolution of 3, 4 and 5.

In order to quantify the different behaviour of PPL in the asymmetrisation of the prochiral diol 2, as well as in the resolution of the racemic diols ( $\pm$ )-1, ( $\pm$ )-3, ( $\pm$ )-4 and ( $\pm$ )-5, we decided to use the mathematical model proposed by Kroutil *et al.*<sup>65</sup> for sequential two-step asymmetrisation/kinetic resolutions, which is summarised in Scheme 4. In this scheme, *S* is a prochiral (or *meso*) substrate, *P* and *Q* are the enantiomeric products obtained in

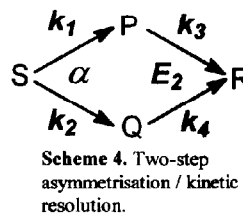
the asymmetrisation step, while *R* is the prochiral (or *meso*) product obtained through the enzymatic kinetic resolution of *P* and *Q*. The selectivity of this type of reaction has been described to be solely governed by the so-called selectivity factor ( $\alpha$ ), which is equal to the ratio of the apparent first-order constants  $k_1$  and  $k_2$ , while  $E_2$  (the ratio of  $k_3$  and  $k_4$ ) is the enantioselectivity ratio of the kinetic resolution. As long as the first step is considered alone, the enantiomeric purity of the product (*P/Q*) is independent of the conversion, although this is not true for the second step, the kinetic resolution, so that for the whole process the enantiomeric excess of the (*P/Q*) mixture does depend on the extent of conversion. The kinetics of the overall process are defined by the following equations:

$$S = S_0 e^{-(k_1+k_2)t} \quad [1]$$

$$P = S_0 \frac{k_1}{k_3(k_1+k_2)} [e^{-(k_1+k_2)t} - e^{-k_3t}] \quad [2]$$

$$Q = S_0 \frac{k_2}{k_4(k_1+k_2)} [e^{-(k_1+k_2)t} - e^{-k_4t}] \quad [3]$$

$$R = S_0 - S - P - Q \quad [4]$$



Thus, by simply calculating these constants from the fittings shown in Figure 1, the values of  $\alpha$  and  $E_2$  for the PPL-catalysed asymmetrisation of **2** could be estimated. If we try to fit the curves obtained for the resolution of the racemic diols (Figure 2) with this same model, some similar constants can be obtained, but now with different meanings, which can be envisaged as follows (taking Scheme 3 as reference):

$E_{1R} = (k_{1R} / k_{1S})$  and  $E_{2R} = (k_{2R} / k_{2S})$  represents the enantioselectivity ratios for the formation of the major and minor monoacetates (acetoxy group further or closer from the stereocentre, respectively).

$E_{DIAC} = (k_{3S} + k_{4S}) / (k_{3R} + k_{4R})$  would quantify the enantioselectivity of the diacetates, because it describes the ratio between the two pathways leading to them.

$rr = (k_{1R} + k_{1S}) / (k_{2R} + k_{2S})$  stands for the regioselectivity ratio, as a quantification of the overall ratio between the formation of the major and minor monoacetates.

Table 1  
Kinetic constants for the PPL-catalysed Transesterification of (1,n)-diols.

PROCHIRAL DIOL												
diol	$k_1, h^{-1}$	$k_2, h^{-1}$	$\alpha$	$k_3, h^{-1}$	$k_4, h^{-1}$	$E_2$						
<b>2</b>	$2.2 \times 10^{-1}$	$1.8 \times 10^{-2}$	12.3	$4.2 \times 10^{-3}$	$3.2 \times 10^{-2}$	0.13						
RACEMIC DIOLS												
diol	$k_{1R}, h^{-1}$	$k_{2R}, h^{-1}$	$k_{3R}, h^{-1}$	$k_{4R}, h^{-1}$	$k_{1S}, h^{-1}$	$k_{2S}, h^{-1}$	$k_{3S}, h^{-1}$	$k_{4S}, h^{-1}$	$E_{1R}$	$E_{2R}$	$E_{DIAC}$	RR
<b>1</b>	$5.5 \times 10^{-2}$	0	0	0	$1.7 \times 10^{-2}$	0	0	0	3.2	---	---	$\infty$
<b>3</b>	$9.0 \times 10^{-2}$	0	$1.3 \times 10^{-3}$	0	$7.1 \times 10^{-2}$	$7.6 \times 10^{-2}$	$2.9 \times 10^{-2}$	$8.0 \times 10^{-3}$	1.3	$\infty$	29	2.1
<b>4</b>	$1.4 \times 10^{-1}$	0	$1.8 \times 10^{-2}$	0	$5.4 \times 10^{-2}$	$5.7 \times 10^{-2}$	0	$5.5 \times 10^{-2}$	2.6	$\infty$	3.1	25
<b>5</b>	$6.9 \times 10^{-2}$	$6.9 \times 10^{-2}$	0	$3.6 \times 10^{-3}$	$6.1 \times 10^{-2}$	$4.0 \times 10^{-2}$	0	$1.1 \times 10^{-2}$	1.1	1.1	3.1	1.2

The values of the constants and these three parameters are shown in Table 1. The acylation of the prochiral diol 2 leads to a *R*-enriched monoacetate 7, because only traces of *S*-7 (< 5%) were detected. So, in order to explain the formation of 8, we assume the double-step kinetics shown in Scheme 2. In these kind of processes, an “opposite” selectivity is always observed for the second kinetic step compared to that of the first step.<sup>1,65</sup> that is, if  $k_1 \gg k_3$ , then  $k_4 \gg k_2$ . This would mean that 8 is formed mainly from the *S*-monoacetate, which is transformed into 8 so quickly that the accumulation of *S*-7 is impossible (and, because of this fact, only traces of *S*-7 are obtained), ( $k_4 \gg k_2$ ). The formation of 8 from the *R*-monoacetate is produced only when the first acylation step is reaching the end, and, because of this fact, the concentration of *R*-7 decreases at long reaction times, as experimentally observed (Figure 1). This means that  $k_7 \gg k_3$ . Thus, PPL displays an excellent asymmetrisation capability, and the best enantiomeric excess of the *R*-monoacetate would be obtained by simply stopping the reaction before its consumption gets noticeable ( $t = [1/(k_3 - (k_1 + k_2))] \times \ln[k_3/(k_1 + k_2)]$ ,<sup>65</sup> 17.2 hours).

If we try to explain the first acylation of the racemic diols, we observe how  $k_{1R} > k_{1S}$  in all the diols, that is, there is a slightly higher *R*-stereobias in the discrimination between the major monoacetates, which is reversed (*S*-stereopreference) if we consider  $k_{2S}$  and  $k_{2R}$ , except for the resolution of 5. On the other hand,  $k_{1R} > k_{2R}$ , while  $k_{2S} \geq k_{1S}$ , that is, the process leading to the major monoacetates is faster than that leading to the minor ones, specially for 4 ( $r = 25$ ). It is noticeable that  $k_{2R} = 0$  for 1, 3 and 4, (no formation of minor *R*-monoacetates), which obviously imply that  $k_{4R} = 0$  in these cases. In the *S*-reaction pathway (Scheme 3)  $k_{3S} = 0$  for 4 and 5. This fact is indicating that these *S*-major monoacetates do not suffer a second acylation process.

If we try to explain the second acylation, we must consider that the diacetates can be obtained through two different pathways, that is, from the acylation of both the major and the minor monoacetates, so that in Table 1, for quantifying the enantioselectivity of this second step, we must use  $E_{D14C}$ . On the other hand, the second acylation is governed by the first step, as we indicated in the previous paragraph. As a general rule we could establish that this second acylation step is generally slower than the first one.

The results obtained for the enzymatic transesterification of the different (1, *n*)-diols are thus demanding a qualitative explanation of the mechanism of the enantiorecognition for this enzyme.

#### Proposal of a Qualitative Model for the Interpretation of the PPL Regio- and Stereoselectivities

With this aim, in order to explain the good regioselectivity in the enzymatic acylation of the OH groups furthest from the stereocentre, the minimum-energy conformers of the different (1, *n*)-diols (represented in Figure 3) were calculated using the HYPERCHEM program<sup>66</sup> (with an AMBER Force Field, and Fletcher-Reeves algorithms (RMS gradient of 0.01 kcal/(Å mol)) to minimize the energy), and were compared with the dimensions of the PPL active site, recently described in literature.<sup>29,30</sup> Figure 4 shows the geometry of the active site of this enzyme, (taken from the PDB structure of the enzyme) highlighting two of the three essential residues from the catalytic triad (Ser153 and His264) as well as Phe216.

Thus, it is possible, according to the dimensions shown in this figure, to postulate the enzymatic recognition of the substrates as caused by a face to face  $\pi$ - $\pi$  stacking interaction between Phe216 and the aromatic moiety of the substrates, as well as by the creation of hydrogen bonds between the non-acylated hydroxy group of the diol and the imidazole ring of His264. With these interactions, the -OH group to be acylated should be placed near the acylated Ser 153 (“chemical operator”). This hypothesis is solidly based on literature data, because from the study of the crystalline structure of different pancreatic lipases (human<sup>67,68</sup> and porcine<sup>29,30</sup>) complexed with different

substrates or inhibitors, it can be noticed how in all cases the only residue of the active site that suffers a change upon

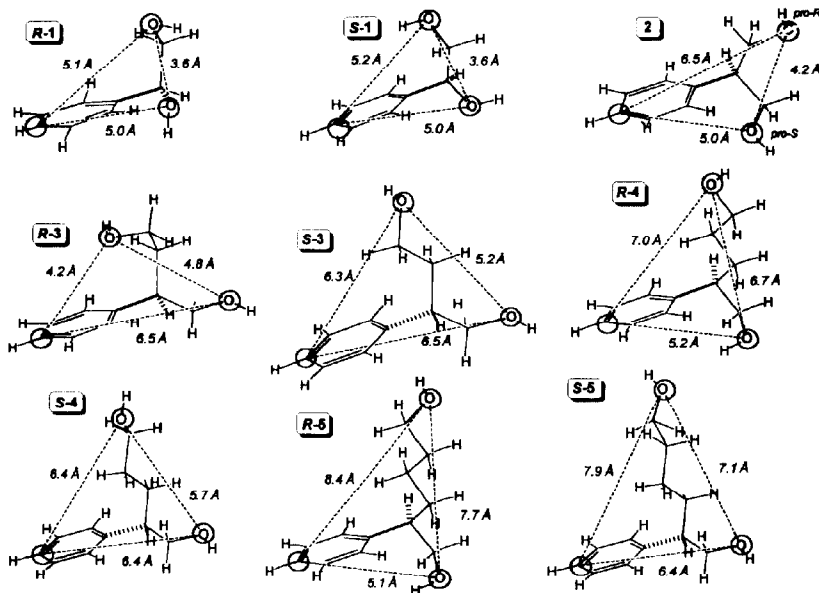


Figure 3. Minimum energy conformers of the different (1,n)-diols.

binding with the inhibitors is Phe216 for pancreatic lipase<sup>29,30</sup> and its equivalent residue Phe215 for human lipase.<sup>67,68</sup> Therefore, these facts indicate the crucial role of this residue for the correct binding of the substrates. On the other hand, in literature some other evidences can be found for the interaction (face to face  $\pi$ - $\pi$  stacking) of aromatic residues nearby the active sites of lipases with the aromatic moiety of different substrates, e.g., 2-aryl or 2-aryloxipropionic acids with Trp-88 residue of *Rh. miehei* lipase<sup>69</sup> or with Phe216 for *C. rugosa* lipase.<sup>68,70</sup> Furthermore, the interaction of substrates with His263 of human pancreatic lipase (equivalent to His264 for the porcine lipase) have also been described<sup>67</sup> via a hydrogen bond between oxygen atoms of inhibitors and the N $\epsilon$  of the imidazole ring.

In order to confirm this hypothesis, as a preliminary step before running any Molecular Dynamics protocol, the previously (in vacuum) minimized structure of R-3 was inserted into the

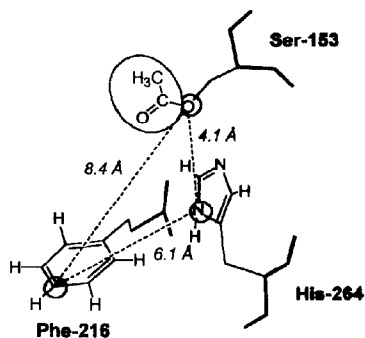


Figure 4. Distances between Ser153, His264 and Phe216 in the active site of PPL, according to the literature<sup>29,30</sup>.



active site pocket, maintaining the reported geometries of the complex pancreatic lipase-substrate.<sup>29,30,67,68</sup> The results obtained with the graphic program O<sup>71</sup> are shown in Figures 5 and 6. Thus, Figure 5 shows the different polarity of the enzyme microenvironments in a colour code (green=hydrophobic, blue= hydrophilic), with the aromatic ring of the substrate interacting with the Phe216, with both -OH groups orientated towards the huge hydrophilic cavity containing the active Ser153 and His264. Figure 6 shows this interaction in more detail, with the correct orientation of the hydroxy group to be acylated approaching the acylated serine.

The geometry requirements for a molecule to be recognized in the active site must be those allowing the correct orientation and the correct distances between the aromatic ring and both hydroxy groups, therefore mimicking those existing in the active site. Thus, using our qualitative model, the high regioselectivity in the acylation of ( $\pm$ )-**1** can be understood comparing their distances (shown in Figure 3) with those of the active site (Figure 4). As represented in Figure 7, the acylation takes place only at the primary alcohol because it is the only possibility for the correct fit: in fact, in the hypothetical acylation of the secondary -OH group (Figure 7B), while the distance between the aromatic ring and the primary -OH (5.1 Å) could emulate that one between Phe216-His264 (6.1 Å), the distance between the aromatic ring and the secondary -OH (5Å) is absolutely fixed because of the complete lack of conformational flexibility of that moiety, and this distance would never be close to that required for the acylation (around 8.4 Å, according to Figure 4). On the contrary, the acylation of the primary alcohol of **R-1** (Figure 7A) would be produced because this -OH group can reach the acylated serine without any problem.

For the rest of the substrates shown in Figure 3, their conformational flexibility would allow them to be acylated in the active site on both hydroxy groups, although the preference observed in the transformation of the longer hydroxyalkyl chain is produced by the best matching of the distance between the aromatic ring and the shorter hydroxyalkyl moiety and the

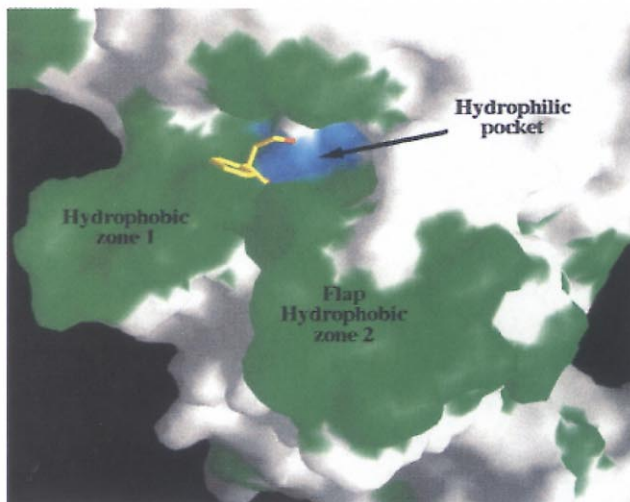


**Figure 5.** Graphical representation of the interaction of **R-3** with the active site of the PPL. Colour code: green= hydrophobic residues, blue= hydrophilic residues. The calculation was carried out with the O program,<sup>71</sup> and presented using the GRASP program.<sup>72</sup>

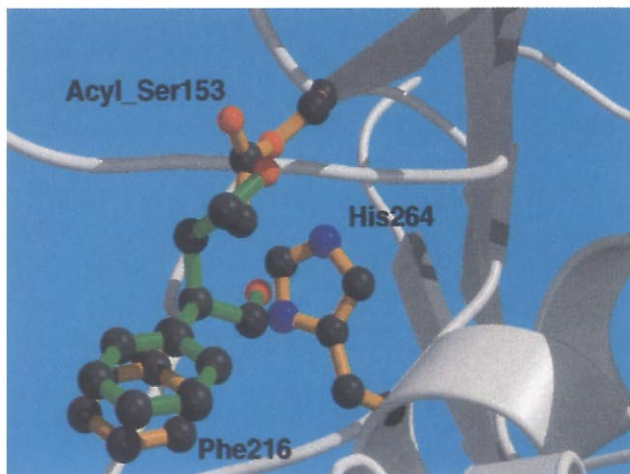


**Figure 6.** Detailed representation of the interaction of **R-3** with the active site of the PPL. Depicted using the MOLSCRIPT program.<sup>73</sup>

distance between the residues Phe216 and His264; this first recognition of the substrates would enable the larger hydroxyalkyl chain to rotate and flex to reach the acylated serine. This is possible due to the large dimensions of the hydrophilic cavity shown in Fig. 5.

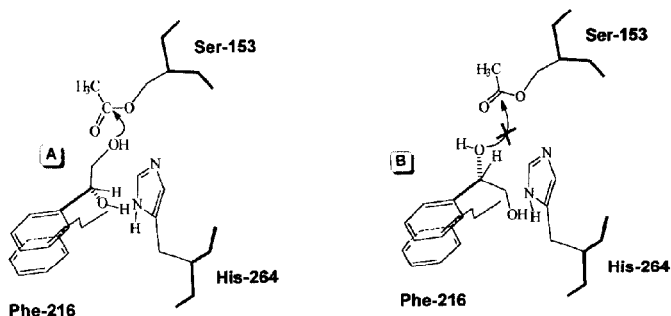


**Figure 7.** (A) Acylation of *R*-1 through the longer hydroxyalkyl moiety (permitted). (B) Acylation of the shorter hydroxyalkyl moiety (not permitted).

Good enantioselectivities are obtained only for the monoacetate *R*-7 (Figure 1) and the minor monoacetates *S*-9 and *S*-12. Nevertheless the high optical purity of *S*-9 and *S*-12 may be caused by kinetic reasons due to the low concentration detected, and fitting **2** in the active site would be the most appropriate, because of the distances between the three points that we are using as references are very similar to the triangle of the active site. The first acylation of **2** takes place on the *pro-R* hydroxy group because, as can be seen in Figure 3, even in vacuum (where the modelling of the substrates was carried out), both -OH groups are not placed at the same distance from the aromatic ring, and therefore the substrate does not have to suffer any distortion when reaching the active site. We think that this is the reason why PPL is the most effective catalyst for the enantiotopic asymmetrisation of 2-substituted 1,3-propanediols.<sup>48-50</sup> As we said before, in the resolution of ( $\pm$ )-**1**, the second acylation of *R*-6 and *S*-6 to form the corresponding diacetates is not observed. This is caused by the excessively short distance between the phenyl ring and the secondary hydroxy group, which impedes this OH reaching the acylated serine, as depicted in Figure 7B.

As shown in Figure 8, the stereobias observed in the PPL-catalysed transesterification of (1,*n*)-diols would favour the previously reported model *A* of the PPL active site proposed for hydrolytic processes by Wimmer<sup>28</sup> (Figure 8B), assuming that the benzene ring is the apolar residue and the hydroxyalkyl group which will not be acylated in the first enzymatic step is the polar moiety; on the other hand, the model defined by Guanti *et al.*<sup>17</sup> (Figure 8C) for the hydrolysis of different *Z* or *E*-alkenyl-1,3-diacetoxypropanes could also be explained in terms of our active site study, which is depicted in Figure 8A, where we propose the residues which would be correlated with the classical subsites models.

Thus, from all the experimental results presented, we propose the following criteria for determining the correct fitting of the diols in the enzymatic active site, based upon its structure:

- a.* - Correct orientation of the longer hydroxyalkyl moiety facing the acylated serine and the shorter one facing His264. This criterium would explain the regioselective acylation of the -OH group further from the stereocenter.
- b.* - Correct orientation of the phenyl group over the Phe216, which would lead to mainly *R* compounds in the first acylation (monoacetates) and *S*-compounds in the second step (diacetates).

For the second step in the acylation (leading to the diacetates) the criteria are not that straightforward. Although it seems clear that an acetoxyalkyl group can be also recognized in the polar subsite (His264), as described,<sup>17</sup> this recognition must be poorer than that observed for a hydroxyalkyl moiety, because the second acylation step generally proceeds more slowly than the first one. Nevertheless this could induce some modifications of the previously mentioned criteria due to the fact that upon changing  $-\text{CH}_2\text{-OH}$  by  $-\text{CH}_2\text{-OAc}$  the interaction with His 264 would be different.

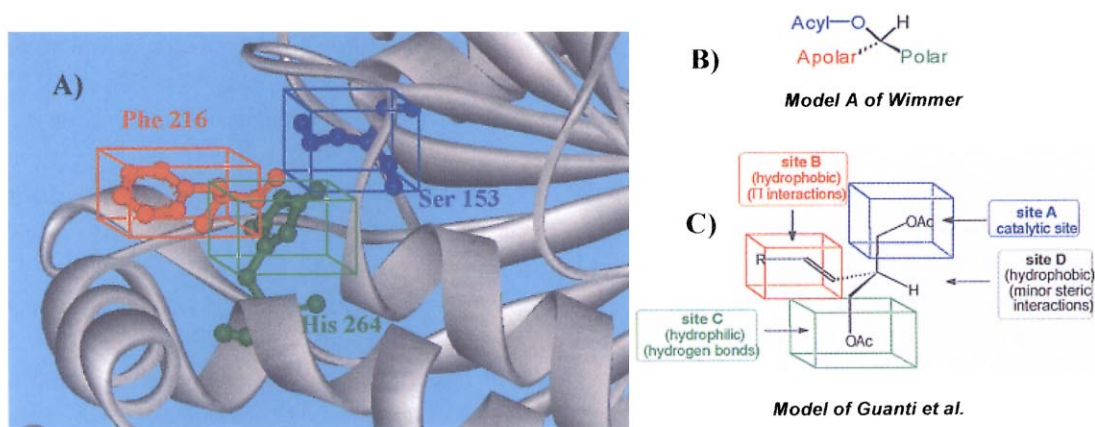


**Figure 8.** Active site “box” model, where the different subzones proposed in the literature by Wimmer<sup>28</sup> (B) and Guanti *et al.*<sup>17</sup> (C) are assigned in the microcrystalline structure of the enzyme (A).

As a final conclusion, we have proposed a rational hypothesis for understanding the enzymatic recognition of substrates for PPL, and located the residues responsible for the lipase regio and stereobias. In order to confirm all these hypothesis, different experiments of Molecular Dynamics, minimizing the enzyme-substrate transition state binding energies, are currently in progress.

### Experimental Section.

**Materials** Lipases (E.C.3.1.1.3.) from Porcine Pancreas, crude (Steapsin), type II, and purified, type VI, were obtained from Sigma. The racemic alcohol ( $\pm$ )-**1** and all the reagents and solvents used were purchased from Aldrich Chemical Co., Alcobendas, Spain.

**PPL-Catalyzed Transesterification of Racemic 2-Phenyl-1,n-alkanediol: General Procedure** A solution of diols **1-5** (6 mmol) and vinyl acetate (48 mmol, 4.4 ml), in diisopropyl ether (15 ml) was stirred at 25 °C with PPL (300mg commercial powder). Then, aliquots of 0.1 ml were taken from the solution (at different times) and added to 0.9 ml of a 80/20 n-hexane/isopropanol mixture; after microfiltration, they were analyzed by HPLC. The spectrophotometrical quantification ( $\lambda=254$  nm) of products concentration and the enantiomeric excess of the products were calculated using an external standard method.

Analysis conditions for the products were as follows:

- For the resolution of mixtures of ( $\pm$ )-**1**, **R-6** and **S-6**: isocratic mixture of n-hexane/isopropanol (97/3), flow

rate=0.7 ml/min (P=400 psi). Retention time: **S-1**, t= 46 min; **R-1**, t= 41 min; **R-6**, t= 34 min; **S-6**, t=30 min.

ii) For the resolution of mixtures of **2**, ( $\pm$ )-**7** and **8**: isocratic mixture of n-hexane/isopropanol (97/3), flow rate=0.7 ml/min (P=400 psi). Retention times: **2**, t=34 min; **R-7**, t=24 min; **8**, t= 13 min.

iii) For the resolution of mixtures of ( $\pm$ )-**3**, **R-10**, **S-10**, **S-9**, **R-11** and **S-11**: n-hexane/isopropanol gradient: t=0 min, flow rate=0.5 ml/min, 98/2 n-hexane/isopropanol; t=30 min, flow rate=1 ml/min, 97/3 n-hexane/isopropanol. Retention times: **R-3**, t=58 min; **S-3**, t=56 min; **R-10**, t= 42 min; **S-10**, t= 40 min; **S-9**, t=48 min; **R-11**, t= 28 min; **S-11**, t=21 min.

iv) For the resolution of mixtures of ( $\pm$ )-**4**, **R-13**, **S-13**, **S-12**, **R-14** and **S-14**: n-hexane/isopropanol gradient: t=0 min, flow rate= 0.5 ml/min, 98/2 n-hexane/isopropanol; t=25 min, flow rate= 0.6 ml/min, 97/3 n-hexane/isopropanol; t=29 min, flow rate=1 ml/min, 97/3 n-hexane/isopropanol. Retention times: **4**, t=57 min (only one peak); **13**, t= 40 min (only one peak); **S-12**, t=46 min; **R-14** , t=22 min; **S-14**, t=20 min.

v) For the resolution of mixtures of ( $\pm$ )-**5**, **R-16**, **S-16**, **R-15**, **S-15**, **R-17** and **S-17** the same above mentioned solvents gradient was used. Retention times: **S-5**, t=68 min; **R-5**, t=64 min; **S-16**, t=47 min; **R-16**, t=45 min; **S-15**, t=53 min; **R-15**, t=50 min, **S-17**, t=19 min; **R-17**, t=17 min.

At a convenient fixed reaction time, the crude reaction mixture, after removal of the enzyme by filtration, was concentrated and the remaining residue was chromatographically separated on a silica gel column (hexane: EtOAc 1:2), obtaining fractions containing the monoacetates (major and minor), the diacetates and the remnant diols, which structures were confirmed by <sup>1</sup>H-NMR and <sup>13</sup>C-NMR and microanalysis. The absolute configuration of the reaction product was established as described in a previous paper.<sup>31</sup>

#### Acknowledgment

This work was financially supported by the projects QUI97-0506-C03- 03 (CICYT) and PR49198-7794 (UCM). I. Borreguero thanks the Comunidad Autónoma de Madrid for the support of a PhD fellowship. We would like to thank Ashley M. Seaman for his critical reading of this manuscript.

#### REFERENCES

1. Faber, K. *Biotransformations in Organic Chemistry*; Springer-Verlag: Heidelberg, 1992.
2. Wong, C. H.; Whitesides, G. M. *Enzymes in Synthetic Organic Chemistry*; Elsevier Sci., Ltd.: Trowbridge, 1994.
3. Drauz, K.; Waldmann, H. *Enzyme Catalysis in Organic Synthesis*; VCH: Weinheim, 1995.
4. Theil, F.; Lemke, K.; Ballschuh, S.; Kunath, A.; Schick, H. *Tetrahedron: Asymmetry* 1995, 6, 1323-1344.
5. Lemke, K.; Theil, F.; Kunath, A.; Schick, H. *Tetrahedron: Asymmetry* 1996, 7, 971-974.
6. Di Bussolo, V.; Catelani, G.; Mastorilli, E.; Di Bugno, C.; Giorgi, R. *Tetrahedron: Asymmetry* 1996, 7, 3585-3592.
7. Guanti, G.; Riva, R. *Tetrahedron: Asymmetry* 1995, 6, 2921-2924.
8. Ferraboschi, P.; Casati, S.; Verza, E.; Santaniello, E. *Tetrahedron: Asymmetry* 1995, 6, 1027-1030.
9. Theil, F. *Tetrahedron: Asymmetry* 1995, 6, 1693-1698.
10. Nair, M. S.; Anilkumar, A. T. *Tetrahedron: Asymmetry* 1996, 7, 511-514.
11. Eguchi, T.; Mochida, K. *Biotechnol. Lett.* 1993, 15, 955-960.
12. Banfi, L.; Guanti, G.; Riva, R. *Tetrahedron: Asymmetry* 1995, 6, 1345-1356.
13. Levayer, F.; Rabiller, C.; Tellier, C. *Tetrahedron: Asymmetry* 1995, 6, 1675-1682.
14. Lemke, K.; Lemke, M.; Theil, F. *J. Org. Chem.*, 1997, 62, 6268-6273.
15. Ramadas, S.; David Krupadanam, G. L. *Tetrahedron: Asymmetry* 1997, 8, 3059-3066.
16. Nguyen, B. V.; Nordin, O.; Vörde, C.; Hedenström, E.; Högberg, H. E. *Tetrahedron: Asymmetry* 1997, 8, 983-986.
17. Guanti, G.; Banfi, L.; Narisano, E. *J. Org. Chem.* 1992, 57, 1540-1554.

18. Carrea, G.; De Amici, M.; De Micheli, C.; Liverani, P.; Carnielli, M.; Riva, S. *Tetrahedron* **1993**, *41*, 1063-1072.
19. Weissfloch, A. N. E.; Kazlauskas, R. J. *J. Org. Chem.* **1995**, *60*, 6959-6969.
20. Cygler, M.; Grochulski, P.; Kazlauskas, R. J.; Schrag, J. D.; Bouthillier, F.; Rubin, B.; Serrequi, A. N.; Gupta, A.K. *J. Am. Chem. Soc.* **1994**, *46*, 3180-3186.
21. Uppenberg, J.; Ohmer, N.; Norin, M.; Hult, K.; Kleywegt, G. J.; Patkar, S.; Waagen, V.; Anthonsen, T.; Jones, T. A. *Biochemistry* **1995**, *34*, 16838-16851.
22. Holmquist, M.; Haeflner, F.; Norin, T.; Hult, K. *Protein Sci.* **1996**, *5*, 83-88.
23. Berglund, P.; Holmquist, M.; Hult, K. *J. Mol. Catal. B: Enzymatic* **1998**, *5*, 283-287.
24. Rotticci, D.; Haeflner, F.; Orrenius, C.; Norin, T.; Hult, K. *J. Mol. Catal. B: Enzymatic* **1998**, *5*, 267-272.
25. Zuegg, J.; Höning, H.; Schrag, J. D.; Cygler, M. *J. Mol. Catal., B: Enzymatic* **1997**, *3*, 83-98.
26. Ehrler, J.; Seebach, D. *Liebigs Ann. Chem.* **1990**, 379-388.
27. Hultin, P. G.; Jones, J. B. *Tetrahedron Lett.* **1992**, *33*, 1399-1402.
28. Wimmer, Z. *Tetrahedron* **1992**, *48*, 8431-8436.
29. Hermoso, J.; Pignol, D.; Kerfelec, B.; Crenon, I.; Chapus, C.; Fontecilla-Camps, J. C. *J. Biol. Chem.* **1996**, *271*, 18007-18016.
30. Hermoso, J.; Pignol, D.; Penel, S.; Roth, M.; Chapus, C.; Fontecilla-Camps, J. C. *EMBO J.* **1997**, *16*, 5531-5536.
31. Rumbero, A.; Borreguero, I.; Sinisterra, J.V. and Alcántara, A.R. *Tetrahedron*. **1999**. Preceding paper.
32. Denis, J. N.; Correa, A.; Greene, A. E. *J. Org. Chem.* **1990**, *55*, 1957-1959.
33. Wang, Z. M.; Kolb, H. C.; Sharpless, K. B. *J. Org. Chem.* **1994**, *59*, 5104-5105.
34. Kwong, H. L.; Sorato, C.; Ogino, Y.; Chen, H.; Sharpless, K. B. *Tetrahedron Lett.* **1990**, *31*, 2999-3002.
35. Kolb, H. C.; van Nieuwenhze, M. S.; Sharpless, K. B. *Chem. Rev.* **1994**, *94i*, 2483-2547.
36. Fan, Q. H.; Yeung, C. H.; Chan, A. S. C. *Tetrahedron: Asymmetry*. **1997**, *8*, 4041-4045.
37. Parida, S.; Dordick, J. S. *J. Am. Chem. Soc.* **1991**, *113*, 2253-2259.
38. Kim, M. J.; Choi, Y. K. *J. Org. Chem.* **1992**, *57*, 1605-1607.
39. Lee, D.; Kim, M. J. *Tetrahedron Lett.* **1998**, *39*, 2163-2166.
40. Bianchi, D.; Bosetti, A.; Cesti, P.; Golini, P. *Tetrahedron Lett.* **1992**, *33*, 3231-3234.
41. Ortu, R. V. A.; Mayer, S. F.; Kroutil, N.; Faber, K. *Tetrahedron* **1998**, *54*, 859-874.
42. Archelas, A. *J. Mol. Catal. B: Enzymatic*, **1998**, *5*, 79-85.
43. Theil, F. *Catalysis Today*, **1994**, *22*, 517-536.
44. Parmar, V. S.; Sinha, R.; Bisht, K. S.; Gupta, S.; Prasad, A. K.; Taneja, P. *Tetrahedron*, **1993**, *49*, 4107-4116.
45. Patel, R. N.; Banerjee, A.; McNamee, C. G.; Szarka, L. J. *Tetrahedron: Asymmetry* **1995**, *6*, 123-130.
46. Theil, F.; Weidner, J.; Ballschuh, S.; Kunath, A.; Schick, H. *Tetrahedron Lett.*, **1993**, *34*, 305-306.
47. Weidner, J.; Theil, F.; Schick, H. *Tetrahedron: Asymmetry* **1994**, *5*, 751-754.
48. Alexandre, F. R.; Huet, F. *Tetrahedron: Asymmetry* **1998**, *9*, 2301-2310.
49. Banfi, L.; Guanti, G.; Mugnoli, A.; Riva, R. *Tetrahedron: Asymmetry* **1998**, *9*, 2481-2492.
50. Shishido, K.; Bando, T. *J. Mol. Catal. B: Enzymatic*, **1998**, *5*, 183-186.
51. Campbell, D. R.; Wojciechowski, B. W. *J. Catal.* **1971**, *20*, 217.
52. Johnson, C. R.; Golebiewski, A.; Steensma, D. H. *J. Am. Chem. Soc.* **1992**, *114*, 9414-9418.
53. Moriya, M.; Kamikubo, T.; Ogasawara, K. *Synthesis* **1995**, 187-190.
54. Johnson, C. R.; Bis, S. J. *J. Org. Chem.* **1995**, *60*, 615-623.
55. Trincon, A.; Pagnotta, E. *Tetrahedron: Asymmetry*, **1996**, *7*, 2773-2774.
56. Lampe, T. F. J.; Hoffmann, H. M. R.; Borscheuer, U. T. *Tetrahedron: Asymmetry*, **1996**, *7*, 2889-2900.
57. Matsuo, K.; Tanaka, M.; Sakai, K.; Suemune, H. *Tetrahedron: Asymmetry*, **1997**, *8*, 3089-3094.
58. Chênevert, R.; Desjardins, M. *J. Org. Chem.* **1996**, *61*, 1219-1222.
59. Bremen, U.; Gais, H. J. *Tetrahedron: Asymmetry* **1996**, *7*, 3063-3066.
60. Bonini, C.; Racioppi, R.; Viggiani, L. *Tetrahedron: Asymmetry* **1997**, *8*, 353-354.
61. Roberts, S. M.; Stenkers, V. G. R.; Taylor, P. L. *Tetrahedron: Asymmetry* **1993**, *4*, 969-972.
62. Lemke, K.; Ballschuh, S.; Kunath, A.; Theil, F. *Tetrahedron: Asymmetry*, **1997**, *8*, 2051-2055.
63. Grisenti, P.; Ferraboschi, P.; Casati, S.; Santaniello, E. *Tetrahedron: Asymmetry*, **1993**, *4*, 997-1006.

64. Hsiao, K. F.; Yang, F. L.; Wu, S. H.; Wang, K. T. *Biotechnology Lett.* **1996**, *18*, 1277-1282.
65. Kroutil, W.; Klewein, A.; Faber K. *Tetrahedron: Asymmetry*, **1997**, *8*, 3251-3261.
66. HYPERCHEM V. 5.1 Pro for Windows™. Molecular modeling system. Hypercube, Inc. And Autodesk, Inc., **1997**.
67. Egloff, M. P.; Marguet, F.; Buono, G.; Verger, R.; Cambillau, C.; van Tilbeurgh, H. *Biochemistry*, **1995**, *34*, 2751-2762.
68. van Tilbeurgh, H.; Egloff, M. P.; Martinez, C.; Rugani, N.; Verger, R.; Cambillau, C. *Nature*, **1993**, *362*, 814-820.
69. Botta, M.; Cernia, E.; Corelli, F.; Manetti, F.; Soro, S. *Biochim. Biophys. Acta*, **1997**, *1337*, 302-310.
70. Winkler, F.; D'Arcy, A.; Hunziker, W. *Nature*, **1990**, *343*, 771-774.
71. Jones, T. A.; Zou, J. Y.; Cowan, S. W.; Kjeldgaard, M. *Acta Crystallogr., Sect. B Struct. Sci.*, **1991**, *47*, 110-119.
72. Nicholls, A.; Sharp, K.; Honig, B. *Proteins Struct. Funct. Genet.* **1991**, *11*, 281.
73. Kraulis, P. J. *J. Appl. Crystallogr.*, **1991**, *24*, 946-950.